

¹ Meteorologisches Institut der Universität München, Germany

Genesis conditions for thunderstorm growth and the development of a squall line in the northern Alpine foreland

Maria Peristeri¹, Wolfgang Ulrich¹, and Roger K. Smith¹

With 8 Figures

Received March 9, 1999

Revised July 10, 1999

Summary

Two numerical models are used to investigate aspects of thunderstorm dynamics and thunderstorm initiation in the northern Alpine foreland. The first, an isentropic model of airflow over and around the Alps, is used to investigate flow patterns favourable for the initiation of deep convection in the region. It is found that a stably-stratified southerly flow towards the Alps leads to a southwesterly flow in the Alpine foreland, a situation most often found during thunderstorm periods, and to the formation of a gravity wave in the lee of the Alps. This wave is accompanied by raised isentropes which, in reality, would lead to a reduction in static stability and convective inhibition as well as an increase in convective available potential energy. The second model, a cloud model, is used to study the development of an observed squall line over southern Bavaria. The model is initialized with wind, temperature and moisture profiles from a radiosonde sounding ahead of the squall line and the squall line is initiated by an array of thermal bubbles. The model simulation is used to interpret the evolution of the squall line.

1. Introduction

Severe thunderstorms in the northern Alpine foreland are a common phenomenon in summer. However they are less frequent than their counterparts in the United States and they do not spawn major tornadoes. Nevertheless, storms occasionally reach an intensity sufficient to produce large hail and severe wind gusts, a notable example being the Mu-

nich hailstorm in 1984 (Höller and Reinhardt, 1986). Statistics for storm development in Upper Bavaria show that the Allgäu is a preferred region for thunderstorms, where on average there are 35 thunderstorms days compared with 28 in the Alpine foreland (Pelz, 1984). Since the early nineties several field experiments have contributed to an improved knowledge of thunderstorms in the northern Alpine foreland. In the summer of 1992 the CLEOPATRA experiment was carried out in southern Germany to study aspects of the regional hydrological cycle (Meischner et al., 1993). One component of it was designed to document the structure and evolution of severe thunderstorms that develop north of the Alps. It is hypothesized by Haase-Straub et al. (1997) that such storms develop in southwesterly air streams in early spring and summer when (i) the low-level moisture advection is large north of the Alps, and (ii) the cross-mountain airflow induces low pressure on the northern side of the Alps leading to low-level convergence over Switzerland and Germany. Since then further experiments have followed in the region including the SEevere Thunderstorm EXperiment (SETEX) and the experiments LINOX (Lightning produced NO_x, Höller et al., 1999, Huntrieser et al., 1998) and EULINOX (European Lightning Nitrogen Oxides Project, Höller et al., 1998). Testing the foregoing hypotheses calls for numerical as well as observational studies.

Recently Hagen et al. (1998) analyzed the propagation characteristics of thunderstorms over southern Germany with data from a lightning detection system and showed that thunderstorms normally move from the sector between west and southwest with an average speed of 13 m/s. They found that the synoptic-scale flow pattern characterized by the Grosswetterlage (greater synoptic situation, e.g. Baur 1957) does not provide a good indication of the likelihood of storm genesis. Radiosonde soundings from Munich and Stuttgart were analyzed on thunderstorm days. It was found that higher vertical wind shears favour moving thunderstorms or thunderstorm lines. Relatively high values of convective available potential energy (CAPE) are observed when moving thunderstorms or thunderstorm lines are present. Stationary storms occur in conditions of low wind speed and low vertical wind shear, the latter corresponding with high Richardson numbers. Moving thunderstorms and thunderstorm lines have similar shear values, but thunderstorm lines have higher CAPE values. Hagen et al. found average CAPE values of 700 J/kg for moving thunderstorms and 880 J/kg for thunderstorm lines, assuming pseudoadiabatic parcel ascent from the surface. Within the framework of HERA, Hagen et al. (1999) investigated the tracks of Mesoscale Convective Systems (MCS) along the northern side of the Alps using radar composites. They showed the trajectories of fifteen MCSs obtained from the HERA images in their Figure 3. All move from west to east, nine originated in France, five in Switzerland and one in southwestern Germany.

Until now, very few modelling studies of cases observed in the recent field experiments have been published. Alheit and Hauf (1994) compared the simulation of a single thunderstorm with airborne measurements of the storm. They found that in this case the Munich radiosonde sounding was too dry close to the surface to initiate deep convection. Increasing the low-level moisture (dew point) led to the development of deep convection in their model. They initialized their model thunderstorm by what they termed an entropy bubble, which was turned off after 30 minutes. Their mesoscale model, MESO-SCOP, has a very detailed representation of cloud microphysics.

Doms (1994) reran the Europa Model (EM) of the German Weather Service (DWD) for a squall-line case documented during the CLEOPATRA Experi-

ment. His Fig. 3 for this simulation shows a generally southerly flow at 850 hPa ahead of a frontal system approaching from the west, with southwesterly flow in the northern Alpine foreland. Over the Adriatic Sea however, the flow is from the southeast into the Po-valley, turning around the French Alps into a southwesterly flow over southern Germany. Doms shows also the wind field at 10 m from a simulation of the finer resolution Deutschland Model. Compared with the EM calculation, details emerge in the flow field on account of the finer scale features of the orography, although the wind speed over the central Alps is very weak. The approximate location of flow splitting is near the northern tip of the Adriatic Sea. Doms remarked on the sudden meso- β scale organization of the flow when a prefrontal convergence line moved eastward and crossed Bavaria. Although this simulation was performed with a relatively complete representation of physical processes and showed very good agreement with observations, it has little to say concerning the favourable conditions for convection. These simulations lend support the foregoing hypotheses of Haase-Straub et al. (1997), but the reasons remain unclear.

There are well known general favourable conditions for convection such as low static stability in the boundary layer, low-level convergence, large-scale lifting above the well-mixed layer and large values of CAPE. Often a parcel must overcome a considerable depth of negative buoyancy if it is to rise to its level of free convection (LFC). This negative area, or convective inhibition (CIN), may be reduced or eliminated by surface heating, differential horizontal temperature and/or moisture advection, or lifting of the conditionally-unstable environment. The criteria used to determine when and where deep convection occurs in a numerical model are collectively termed the convective trigger function. Convection schemes such as those based on entraining-plume models require certain local triggers, such as a positive temperature deviation or vertical lifting larger than a certain threshold to become active. Rotunno et al. (1984) investigate the importance of the low-level shear on the maintenance of deep convection. Wind profiles with low-level shear were observed during CLEOPATRA (Peristeri and Smith, 1994) and these may be presumed to be influenced by the presence of the Alps.

In this paper we summarize briefly the results of two idealized numerical modelling studies related

to convective storms in the Alpine region that were carried out as part of the HERA project. In the first, we investigate ways in which the Alps provide favourable conditions for thunderstorm initiation. For this study, described in detail in section 2, we use a simple dry-isentropic model in which the Alps are idealized as a mountain ridge with an elliptical ground plan and the same horizontal scale of the Alps. Since there are no major sources of moisture in the northern Alpine foreland, the moisture supply for storm initiation must be transported by the low-level airflow around the orography. There are many investigations of idealized flow over topography, but most are concerned with gravity wave breaking, lee waves, or upstream blocking. Here we focus on the three-dimensional airflow patterns in the lee of the orography and the low-level lifting produced by the mountain-induced gravity waves, which provides a mechanism for convective destabilization.

In the second modelling study, described in section 3, we use a cloud model to investigate the evolution of a squall-line in the near-Alpine flow environment. The model does not contain orography, but the simulation is influenced indirectly by the proximity of the Alps through the initial sounding used. Because of the model's relative computational efficiency, it is possible to carry out sensitivity studies related to the initial disturbance. Moreover, the simulations can be compared with the fine-scale analyses of observational data (see Peristeri, 1999).

2. Adiabatic flow over idealized Alpine topography

2.1 The numerical model

To investigate the basic flow patterns that might favour deep convection in the northern Alpine foreland, we use a three-dimensional isentropic model in a rotating channel, similar to that of Bleck (1984). A concise documentation of the model can be found in Bauer (1997). Isentropic layers are allowed to collapse using the so-called massless layer approach (see Bleck, 1984, for details). At the lower boundary a conventional drag law with a drag coefficient $c_D = 0.001$ is applied. The inclusion of surface drag reduces the tendency for gravity wave breaking in the model and extends the parameter range, especially the range of mountain heights, over which the model can be applied. There is a Rayleigh damping

sponge layer in the upper part of the domain to reduce wave reflection from the top lid.

The model domain is chosen to be 1230 km by 1230 km, which is large enough to encompass the entire Alps including the Alpine foreland, and the Alps are represented by an idealized elevated ridge with elliptical ground plan and parabolic vertical cross-section. The peak height is $h_{max} = 2000$ m and the horizontal dimensions are 600 km by 300 km. Different flow directions are achieved by rotating the ridge. Eight layers are used in the vertical with a potential temperature difference of 6 K between layers. The horizontal grid resolution is 13.5 km. The basic stratification corresponds to a Brunt-Väisälä frequency of $N = 10^{-2} s^{-1}$. All calculations are initialized with a uniform flow of 10 ms^{-1} .

Bauer (1997) carried out a large number of flow experiments with a similar topography, and with another constructed from analytic functions, which has an extra flank representing the Sea-Alps. Thorsteinsson and Sigurdsson (1996) summarized earlier findings on blocking and flow splitting for a mountain with an elliptical ground plan. They focused on the streamline displacement and upstream blocking for a range of values of the three nondimensional parameters: the Rossby number, $Ro = U/(fl_x)$, the dimensionless mountain height, $H = Nh_m/U$, and the nondimensional mountain shape factor, $A = l_y/l_x$. Here l_x and l_y are the lengths of the major and minor axes of the elliptical ground plan, in the x- (along flow) and y-directions, respectively. The first calculation described here corresponds with the point in parameter space $(Ro, H, A) = (1/3, 2, 2)$. Many of the flow characteristics such as upstream influence and flow splitting can be inferred a priori from Thorsteinsson and Sigurdsson's diagrams, which cover the parameter space $Ro = [0..6]$, $H = [0..6]$, $A = [0..6]$, although these diagrams are based on relatively few experiments. Like Thorsteinsson and Sigurdsson's model, our model cannot handle streamline overturning, to which the foregoing authors attribute only minor importance. Each experiment begins with a uniform flow applied impulsively. After a few hours of integration time the flow pattern changes only gradually. The periodic boundary conditions limit the permissible integration time, but this is not a serious restriction, since, in reality, the large-scale flow is never steady for a prolonged period. Most features in the model never become stationary in the strict sense without excessive damp-

ing, but undergo slow fluctuations with time. We display flow fields after 8 hours of integration. Calculations for more general initial conditions would enormously complicate the task of identifying typical flow patterns and such investigations are beyond the scope of this study.

2.2 Flow experiments

For reasons of space we consider here only basic flows from a southerly sector. After several hours of integration, inertial effects are apparent, the low-level airflow being deflected to the left of the basic flow direction along the upwind side of the obstacle, as discussed by Pierrehumbert and Wyman (1984). Southerly flow may be expected to be deflected around the western Alpine rim and turn into southwesterly flow in the northern Alpine foreland, whereas a westerly or easterly basic flow will be more weakly deflected. Such behaviour is reproduced in our calculations, so that we confine the discussion to common features for flows with a southerly component. Figure 1 shows the stream lines in the lowest layer for southerly flow. The subdomain displayed is 1200 km x 800 km wide. The approximate point of flow-splitting is on the

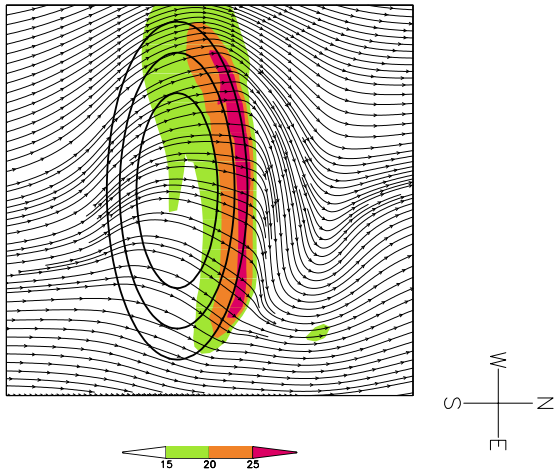


Fig. 1. Stream lines and flow speed (shaded, scale given below figure) in the lowest layer after 8 hours of integration. Basic flow is from the south (from left to right in the figure). The topography is contoured at 500 m intervals. The maximum wind speed reaches 30 m/s.

southeastern rim of the Alps. The deflection of the flow to the southwest and then to west in the north-

ern Alpine foreland and the Foehn-like downslope winds on the northern Alpine rim are prominent features.

Vertical motion may play an important role in enhancing convection (Emanuel, 1994) and vertical windshear is important for maintaining convection (Rotunno et al., 1988). Vertical velocity is not a prognostic variable in the isentropic model and there is no movement of air parcels between layers. Vertical wind shear has its maximum in the model where the flow deflection is largest, north of the Alpine rim.

We investigate now the possible convective destabilization of the airflow. As the potential temperature within a layer is constant, the vertical potential temperature gradient cannot be used as an indicator of stability. An unexplored factor which may also favour convection is the change in thickness of the isentropic layers. A thickening of the lowest isentropic layer by an amount Δh in the flow direction corresponds to a vertical lifting of parcels following the slope of the isentropic interface, and this can be interpreted as relative decrease in stability of the amount $\Delta \theta / \Delta h$. This effect is displayed schematically in a vertical cross-section in Fig. 2. As the

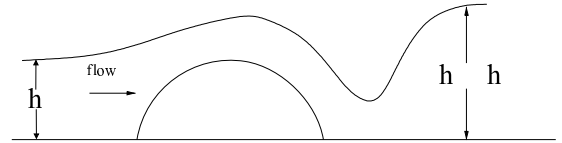


Fig. 2. De-stabilization in the lee of a mountain range by stretching of an isentropic layer. Note that the cross-mountain flow is not in a single vertical plane: this is clear from the horizontal flow patterns in Figs. 1, 4, 5

flow is three dimensional, by virtue of the Coriolis effect, even for a symmetric initial flow conditions with respect to center line of the channel, the cross-section like that in Fig. 2 is to be understood as following the flow over the mountain range. To obtain a three-dimensional view of the proposed stability change, we display the thickness contours of the lowest layer shown in Fig. 3. The idealized Alps are again indicated by bold ellipses. Large thickness values are shaded. There is a gradual ascent of isentropes on the windward side of the Alps. In the lee, a trough has formed downstream of the northeastern rim. The reduced layer thickness within this region would be translated into relatively higher stabilities, thereby favouring suppressed convection. The high

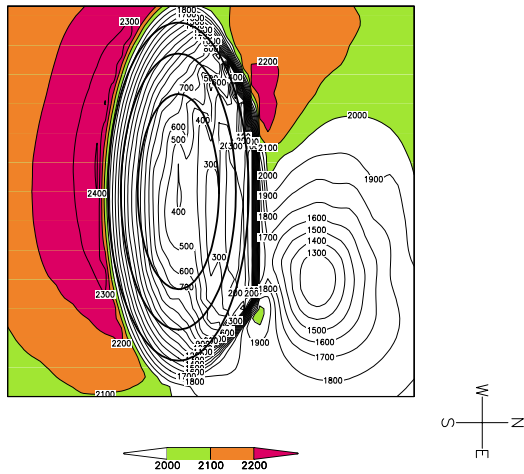


Fig. 3. Thickness of the lowest layer in m after 8 hours of integration corresponding with Fig. 1

thickness values on the northwestern rim, which imply low static stabilities, represent favourable regions for the initiation of convection. It should be noted that the lee cyclone is transient as discussed by Peng et al. (1995) and drifts slowly westwards with the basic flow. Their Fig. 8 may be compared qualitatively with our Fig. 1.

The isentropic model shows that a low-level southwesterly airflow is to be expected north of the Alps when the basic large-scale flow is southerly. This is the case also for southeasterly flow as indicated in Fig. 4 and to a lesser extent for southwesterly flow (Fig. 5). Note that the streamlines and the layer thicknesses are combined in these figures. A flow with a southerly component gives rise to low-level moisture advection from the warm Mediterranean Sea, a feature conducive to thunderstorm initiation. A feature associated with southerly flow favouring the development of convection in the northern Alpine region is the additional destabilization by layer expansion after the relative compression in the lee of the Alps. This effect, which is present in dry and moist models, has the potential to increase the CAPE and reduce the CIN. The actual amount of destabilization for typical upstream temperature and humidity soundings, measured by the actual changes in CAPE and CIN, remains to be quantified.

Recently Schneidereit and Schär (1999) performed numerical experiments in a flow configuration similar to the above with and without moisture

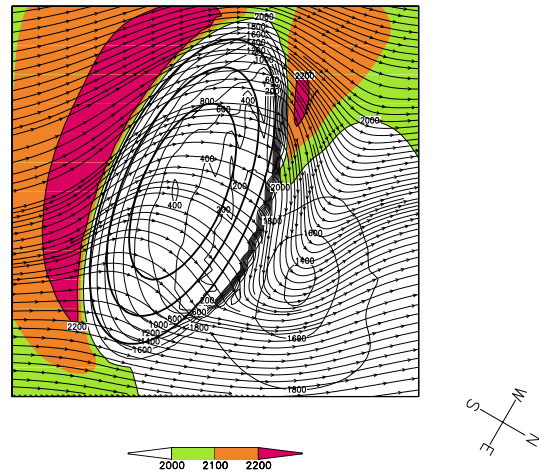


Fig. 4. As Fig. 1 and Fig. 3 combined, but the basic flow is from the south east. The maximum wind speed is very close to 30 m/s.

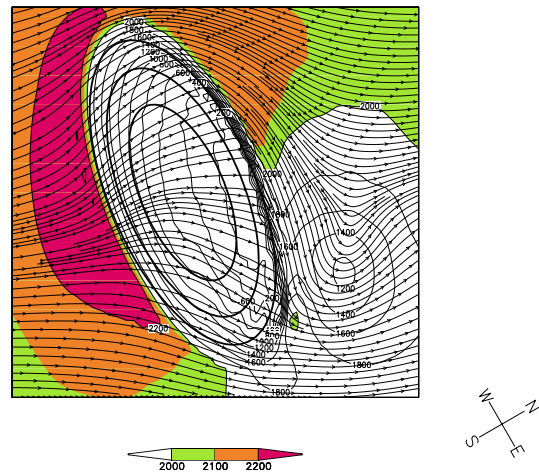


Fig. 5. As Fig. 4, but with the basic flow from the southwest.

(see their Fig. 6). Their calculations do not show a lee-cyclone, although a vortex is generated on the western flank of the Alps. Their flow patterns are difficult to compare with ours, because wind vectors are displayed on the lowest model sigma-surface rather than in isentropic layers. However, their moist experiments show maxima of accumulated precipitation on the upstream slope and at a position in the lee of the Alps, where our calculations predict the largest de-stabilization. Further work is required to establish the importance of the effect described

compared with other mechanisms of destabilization, including orographic triggering. There is observational evidence that some convective systems intensify when crossing the northern Alpine foreland (see Hagen et al., 1999, their Fig. 2), which might be an indirect indicator of de-stabilization in that region.

3. A study of squall line development

3.1 Available data

The SETEX-94 experiment was carried out during the spring and early summer of 1994 in southern Germany and eastern Switzerland with the aim of documenting the formation and evolution of severe thunderstorms in that region. To enable detailed analyses of these systems to be constructed, the routine data (synoptic surface observations, radiosonde soundings and satellite and radar observations) were augmented by extra-operational radar observations and radiosonde soundings as well as a network of 10 automatic weather stations, which covered a large area of southern Bavaria and Baden-Württemberg. An interesting case was observed on 14 July 1994 when a severe thunderstorm developed along a pre-frontal convergence line and caused heavy rainfall in a region north of the Alpine rim. On this day a cold front extending from northern Scandinavia to France was analyzed by the DWD at 0000 UTC. An upper-level ridge over the western Alps induced a north-westerly flow over Bavaria. The convergence line was analyzed about 500 km to the east of the cold front. At 1500 UTC a squall line developed over the northern Alpine region, about 100 km to the east of the convergence line. Subsequently the convergence line drifted eastwards and between 1500 UTC and 1700 UTC it decayed, while the squall line intensified as it moved eastwards.

3.2 The cloud model

Numerical calculations for this event have been carried out using the non-hydrostatic three-dimensional cloud model of Klemp and Wilhelmson (1978). The calculation domain is 280 km in both horizontal directions and 18 km in the vertical, with a horizontal resolution of 2 km and a vertical resolution of 400 m. The initial wind-, potential temperature- and water vapour mixing ratio distributions, displayed in Fig. 6, are taken to be horizontally homogeneous and are based on the radiosonde sounding carried out near

Munich at 1300 UTC on 14 July. Guided by the regional surface analysis at 1300 UTC, a pattern of near-surface thermal bubbles is prescribed at the initial instant in the model to initiate a pattern of convective cells similar to that observed. Model times are referred to in UTC to facilitate comparison with observations. Sensitivity studies showing the evolution of convective systems with different thermal forcing patterns are described in subsection 3.4.

3.3 Control run

The pattern of bubbles for initiating the model squall line is shown in Fig. 7a. The line of bubbles serves to generate convective cells representing the model convergence line and the single bubble to the east initiates the model squall line. After an hour of integration, at 1400 UTC, cold air downdraughts reach the surface, accompanied by a rise in surface pressure. This stage marks the beginning of the formation of the gust fronts and cold pools associated with each bubble. The analysis of observational data at this time shows the development of a high pressure region just behind the southern part of the convergence line. By 1500 UTC, the model gust fronts have spread out and those along the convergence line have merged. During the next hour the gust fronts from the convergence line and the squall line collide and the southern part of the convergence line begins to decay (Fig. 8a). The observational analyses show a further extension of the high pressure area along the southern part of the convergence line and the line itself had decayed. By 1700 UTC the model convergence line has decayed and the squall line, which has further intensified, has moved eastwards, similar to the observed behavior (Fig. 8a). The reason for the demise of the convergence line in the model is the spreading cold pool of both disturbances, which suppresses the development of new convective cells. A rise in surface pressure of 3 hPa associated with the model cold pool was similar to that observed.

3.4 Sensitivity studies

Additional experiments were performed to determine the sensitivity of the flow evolution to the initial distribution of the thermal bubbles. In the first experiment the structure of the initial disturbance is the same as in the control case, but the distance between the line of bubbles and the single bubble is only 20 km instead of 100 km, see Fig. 7b. In this

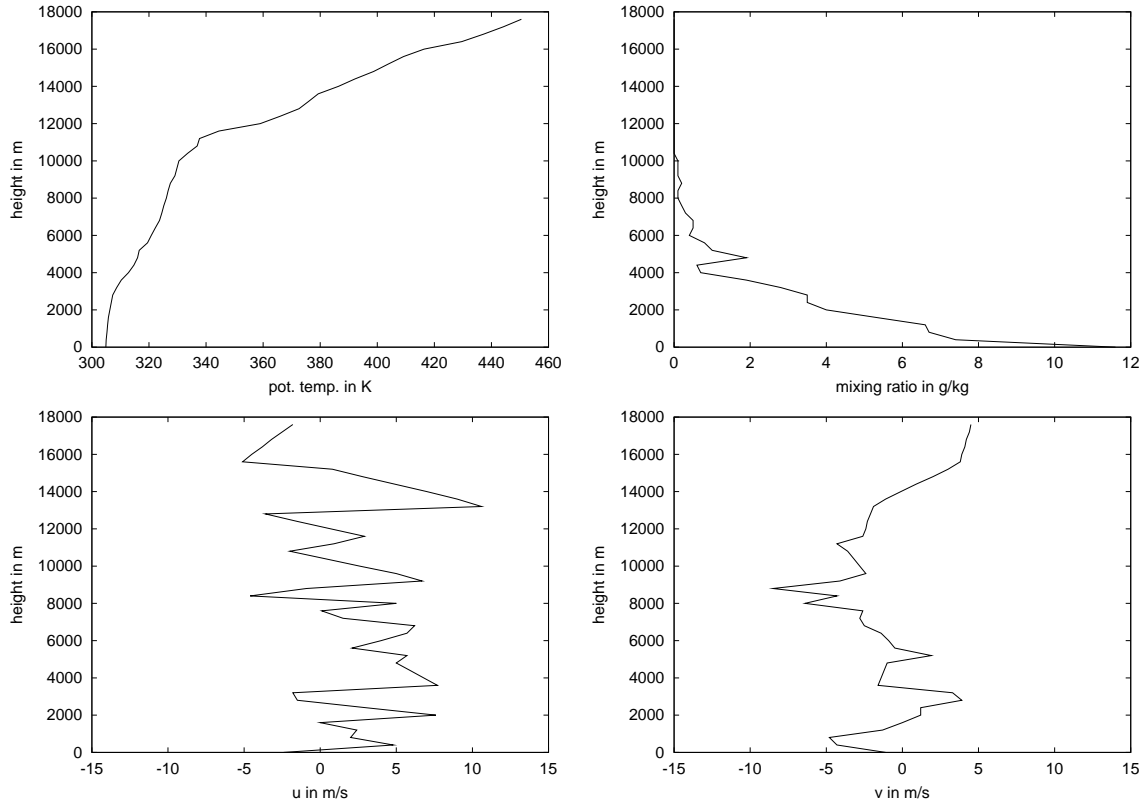


Fig. 6. Radiosonde sounding for the observed case of SETEX. Top left: potential temperature. Top right: mixing ratio. Bottom left and right: zonal (u) and meridional (v) wind components.

case, only the northern part of the convergence line and the single bubble ahead of it developed. The development of the southern part of the convergence line is suppressed by the early development of the gust front and cold pool from the single bubble. The spreading cold pool from this bubble stabilizes the area ahead of the southern part of the convergence line.

In the next experiment, a calculation is carried out with the row of bubbles that represent the convergence line (Fig. 7c), but without the single bubble to the east. Within four hours of integration, strong up- and downdraughts form, but in this case no disturbance develops ahead of the convergence line. Indeed, the line propagates eastwards without decay because of the continued generation of convective cells along its gust front. The air ahead of the line remains unstable to convection because there is no spreading cold pool to suppress the convection as in the control case (Fig. 8c).

In the final experiment, we examine the behaviour

of a single bubble in the domain. In this case a thunderstorm cell develops with weak up- and downdraughts. The cold pool spreads out in all directions and further weak convective cells develop only along the leading edge of the gust front. The system moves to the east, but nothing corresponding to the observed squall line evolves, see Fig. 8d.

These sensitivity studies emphasize the importance of the structure of the initial disturbance for the subsequent flow evolution. While a single cell thunderstorm develops from one initial thermal bubble, a line of bubbles leads to a long-lived convective line. The interaction between two convective systems, which are triggered by different initial thermal bubbles, can lead to a situation where convection is suppressed if the evolution of one of the convective cells is much faster than the other. The reason is the increase in low-level stability along the southern part of the convergence line by the cell to its east, which evolves faster.

In summary, the environment conditions of the

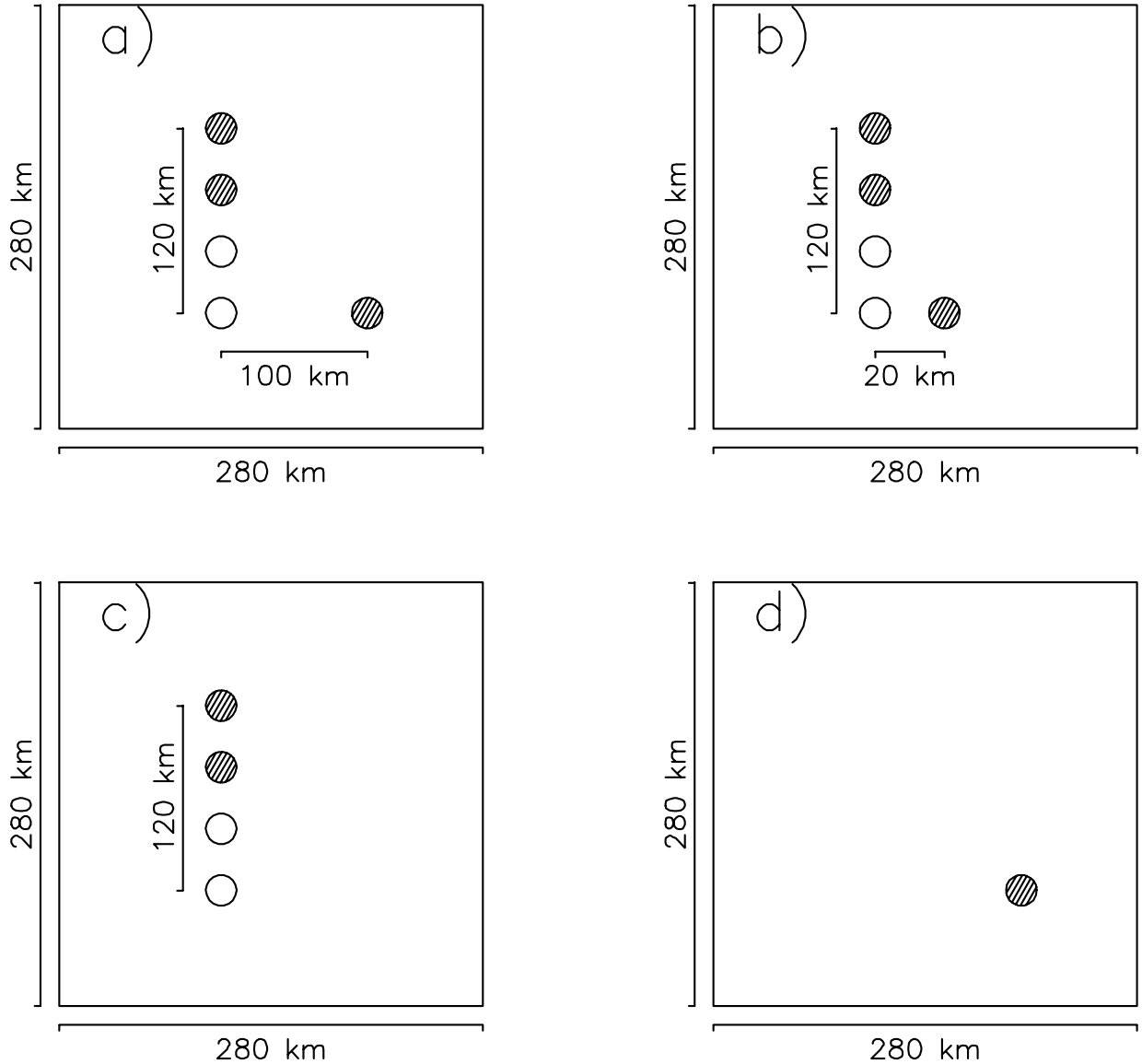


Fig. 7. Schematic description of the initial thermal disturbance related to the squall line event of 14th July 1994 for a) the basic calculation, b) the calculation with a reduced distance between the line and the separated bubble, c) the calculation with a line of bubbles only and d) the calculation for a single bubble only.

SETEX-94 squall-line case favour the development of strong convection after its initiation. The basic ingredients are a low-level wind shear, sufficient CAPE (more than 1000 J/kg) and a CIN that can be surmounted. The structure of the convective system that arises depends also on the pattern of the initial thermal trigger. Interaction between convective cells leads to a weakening of convection, because

the spreading cold pools stabilize the environmental air.

4. Conclusions

We have carried out idealized calculations with two different numerical models to study aspects of convective initiation and evolution in the northern Alpine foreland. We have explored factors con-

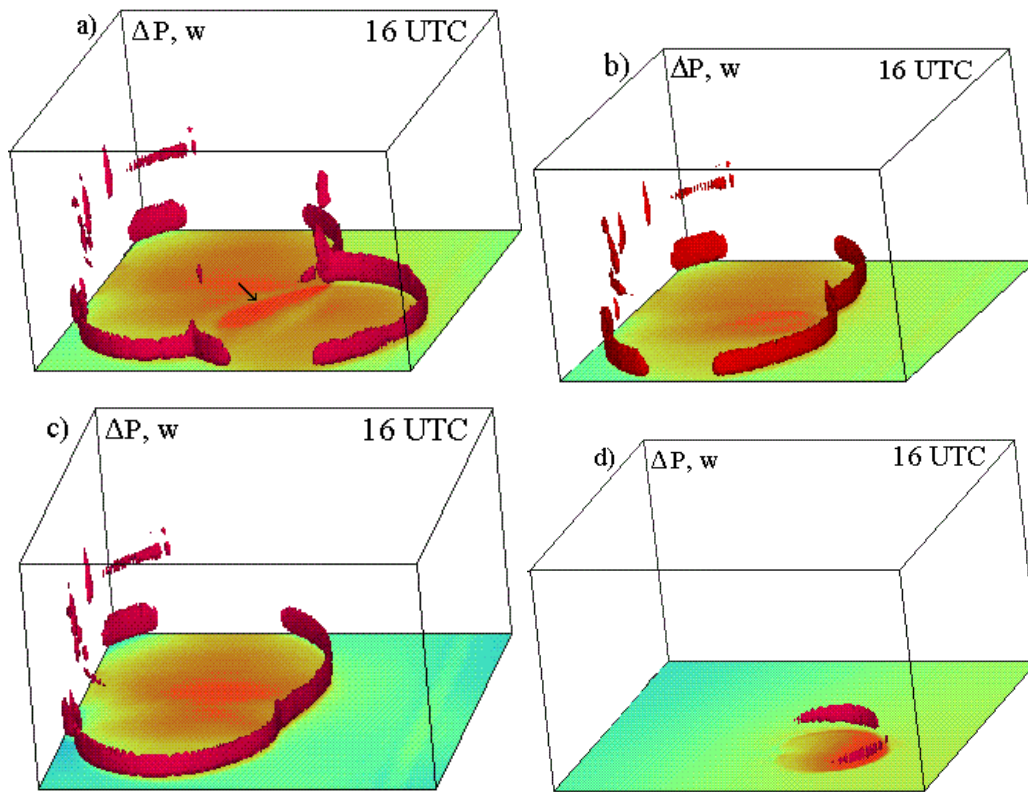


Fig. 8. Three-dimensional depiction of the surface pressure deviation (red corresponds to high pressure, blue with low pressure) and the vertical velocity exceeding 1.36 m/s (arc-shaped banded structures) at 16 UTC: a) Pattern of bubbles corresponds with Fig. 7 a). b) Pattern of bubbles corresponds with Fig. 1b). c) Pattern of bubbles corresponds with Fig. 7c). d) Pattern of bubbles corresponds with Fig. 7 d). The box measures 280 km \times 280 km \times 18 km

ductive for convective initiation in this region using an isentropic-layer model. These factors include a large-scale cross-alpine flow with a southerly component. The isentropic model underlines the important role of the Alps in creating a southwesterly flow in the region and indicates the existence of an area north of the Alps where the isentropes are raised in the mountain-induced gravity wave. The raised isentropes would imply a destabilization of the airstream through a reduction of the CIN and an increase in the CAPE, although the magnitude of these changes remains to be quantified for typical upstream soundings.

Numerical simulations of the evolution of a squall line in the northern Alpine foreland using a cloud model help to interpret the observed evolution of this event, including the decay of a preceding convergence line and the subsequent intensification of the squall line. The decay of the convergence line

was attributed to the merging of the cold pool it produced and the cold pool of the developing storm that later became the squall line. The model was initialized using an observed sounding and a distribution of thermal bubbles constructed on the basis of a surface analysis.

A particularly interesting result of the study is the demonstration that the development of convective systems such as the squall line studied here is significantly influenced by the presence of neighbouring convection. In the calculation described, the growth of a convective cell ahead of the line of cells to its west greatly affects the subsequent evolution of the line. The single cell to the east grows at the expense of the southern part of the line of cells and becomes the dominant feature. In sensitivity studies, where only the line of cells or the single cell were present, the evolution of the convective systems that developed was quite different. The interaction between

storm cells is an area of research that appears to have received relatively little attention in the literature to date.

Acknowledgements

We thank Dr. Morris Weisman at NCAR who allowed to us his version of the cloud model, and Dr. Gisela Hartjenstein who provided her version of the isentropic model. This study was in parts supported by the European Commission, Programme "Environment and Climate" under contract ENV4-CT96-0332.

References

- Alheit, R., T. Hauf, 1994: Observational and modeling study of a thunderstorm ahead a squall line. *DLR-Forschungsbericht 94-18*, 207-221.
- Bauer, M., 1997: Three-dimensional numerical simulations of the influence of the horizontal aspect ratio on flow over and around a meso-scale mountain. *Dissertation, Leopold-Franzens-Universität, Innsbruck, December 1997*.
- Baur, F. (Editor), 1957: Linkes Meteorologisches Taschenbuch. Neue Ausgabe.
- Bleck, R., 1984: An isentropic coordinate model suitable for lee cyclogenesis simulation. *Rivista di Meteorologica Aeronautica*, **4**, 189-194.
- Doms, G, 1994: Numerical simulations with the meso- β -scale model of the DWD. *DLR-Forschungsbericht 94-18*, 179-206.
- Emanuel, K., 1994: Atmospheric convection. *Oxford University Press*, 509-523.
- Haase, S. P., M. Hagen, T. Hauf, D. Heimann, M. Peristeri and R. K. Smith, 1997: The Squall-line of 1992 in Southern Germany: An Observational Case Study. *Beitr. Phys. Atmosph.*, **70**, 147-165
- Hagen, M., B. Bartenschlager, U. Finke, 1998: Propagation characteristics of thunderstorms in southern Germany. *Institut für Physik der Atmosphäre. Report No. 97*.
- Hagen, M., H.-H. Schiesser and M. Dorninger, 1999: Monitoring of mesoscale precipitation systems in the Alps and northern Alpine foreland by radar and rain gauges. Submitted to *Meteor. Atmos. Phys.*
- Juckes, M. and R. K. Smith, 1999: Convective destabilization by upper level troughs. *Q.J.R.Meteorol. in press*
- Klemp, J. B., and R. B. Wilhelmson, 1978: The Simulation of Three-Dimensional Convective Storm Dynamics. *J. Atmos. Sci.*, **35**, 1070-1096.
- Höller, H., U. Finke, H. Huntrieser, M. Hagen, and C. Feigl, 1999: Lightning produced NO_x (LINOX) - Experimental design and case study results. Accepted for publication in *J. Geophys. Res.*
- Höller, H. and M. E. Reinhardt, 1986: The munich hailstorm of July 12, 1984 - Convective development and preliminary hailstone analysis. *Beitr. Phys. Atmosph.*, **59**, 1-12.
- Höller, H., U. Finke, M. Hagen, and H. Huntrieser, 1998: Thunderstorm observations during LINOX - combined radar, satellite, lightning, and in-situ measurements. Proceed. COST 75 Final International Seminar "Advanced Weather Radar Systems", Europ. Commission, Luxembourg, ISBN 92-828-4907-4, 364-374.
- Huntrieser, H., H. Schlager, C. Feigl, H. Höller, 1998: Transport and production of NO_x in electrified thunderstorms: survey of previous studies and new observations in mid-latitudes. *J. Geophys. Res.*, **103**, 28246-28264.
- Meischner, P. E., M. Hagen, T. Hauf, D. Heimann, H. Höller, U. Schumann, W. Jaeschke, W. Mauser and R. H. Pruppacher, 1993: The field project CLEOPATRA, May-July 1992 in Southern Germany. *Bull. Amer. Met. Soc.*, **74**, 401-412.
- Pelz, J., 1984: Die geographische Verteilung der Tage mit Gewitter in Mitteleuropa. *Beilage zur Berliner Wetterkarte 48/84 SO 12/84*, 32 pp.
- Peng, M. S., S.-W. Li, S. W. Chang, and R. T. Williams, 1995: Flow over mountains: Coriolis force, transient troughs and three dimensionality. *Quart. J. Roy. Meteor. Soc.*, **121**, 593-613.
- Peristeri, M., R. K. Smith, 1994: Air-mass analysis using the Penzing radiosonde data. *DLR-Forschungsbericht 94-18*, 27-38.
- Peristeri, M., 1999: Entwicklung von Squall-lines im Alpenvorland. Dissertation an der Fakultät für Physik der Ludwig-Maximilians-Universität München, 176 pp.
- Pierrehumbert R. T. and B. Wyman, 1985: Upstream effects of mesoscale mountains. *J. Atmos. Sci.*, **42**, 977-1003.
- Rotunno, R., Klemp, J. B., and M. L. Weisman, 1988: A Theory for Strong, Long- Lived Squall-Lines. *J. Atmos. Soc.*, **45**, 463-485.
- Schär, C. and M. Schneidereit, 1999: Idealised numerical experiments of Alpine flow regimes and southside precipitation events. Submitted to *Meteor. Atmos. Phys.*
- Thorsteinsson, S and S. Sigurdsson, 1966: Orographic blocking and deflection of stratified air flow on an f-plane. *Tellus*, **48A**, 572-583.

Authors' address: Maria Peristeri, Prof. Dr. Roger K. Smith, Dr. Wolfgang. Ulrich, Meteorologisches Institut der Universität München, D-80333 München, Germany.